

Application of a Joint Source-Channel Decoding Technique to UMTS Channel Codes and OFDM Modulation

Marion Jeanne*, Isabelle Siaud, Olivier Seller and Pierre Siohan

France Télécom R&D, DMR/DDH, Site de Rennes, 4 rue du Clos Courtel,
B.P. 59, 35512 Cesson-Sévigné Cedex, France
{firstname.lastname@francetelecom.com}

Abstract. This paper describes the application of a joint source channel decoding technique (JSCD) of variable length codes (VLCs), presented at first by Guivarch et al., in the context of future public land mobile telecommunication systems (FPLMTS) involving UMTS channel codes and OFDM modulation. OFDM parameter sets have been adjusted both to the UMTS chip rate and to the selectivity of the urban multipath propagation channel. The application of JSCD to UMTS codes may lead to signal to noise improvements greater than 3 dB. A methodology is also proposed to get soft error patterns attached to the transmission system, including the OFDM modulation and the multipath channel. Thus, several JSCD schemes can be accurately evaluated thanks to an equivalent simplified model.

1 Introduction

One of the main objective of FPLMTS is to provide high capacity mobile radio systems allowing the access to various type of high data services, as for instance video. However, to be implemented at a user level the computational complexity and delay involved by these new systems and services have to be relatively low. In the last few years, it has been shown that JSCD techniques could be the right approach to improve the transmission performance given these complexity and delay constraints, see for instance a tutorial introduction by Van Dyck and Miller [1]. In this field, the most recent studies have focused on JSCD methods that could handle the widely spread case of a variable length encoding of the source, as it exists for instance in video encoders. However, most of these techniques have been evaluated with a simple additive white gaussian noise (AWGN) channel [2], [3], and, in some cases on a Rayleigh fading channel [4]. In this paper, the first objective is to evaluate the JSCD proposed in [3] through a mobile radio channel involving UMTS channel codes and an OFDM modulation scheme. Indeed, recent 3GPP investigations on the OFDM modulation for upcoming downlink UMTS-standards on adjacent UMTS-bands [5] have shown its relevance to face the problem of multipath propagation in urban areas. Thus, from a wideband selectivity parameters analysis carried out on simulated outdoor ITU-R models [6] and previous France Telecom measurements [7], we have selected the appropriate ITU-R propagation models.

* This work was supported in part by the French ministry of research under the contract named COSOCATI (http://www.telecom.gouv.fr/rnrt/index_net.html).

In accordance with the UMTS-chip rate, two low-complexity OFDM dimensioning fit with micro and small cell areas, respectively, are defined afterwards. A second objective of our work is to provide a methodology to get soft error patterns files attached to the transmission system. Consequently, a unique soft error pattern can be used to test several JSCD schemes without having to simulate the modulation/demodulation set-up.

Our paper is organized as follows. In section 2 we present the OFDM transmission system. The generation and validation of the soft error pattern are detailed in section 3. Finally, section 4 reports JSCD performance with convolutional codes and turbo codes.

2 The transmission system

2.1 Propagation modelling

Wideband tapped delay line models consist in a discrete version of the scattering function of the propagation channel under wide sense stationary uncorrelated scatterers (WSSUS) assumptions. Hence, the scattering function $P_s(\nu, \tau) = |S(\nu, \tau)|^2$ is a simplified version of the correlation function $R_s(\nu, \nu', \tau, \tau')$ where $S(\nu, \tau)$ is the Doppler-variant channel impulse response of the channel [8] (ν : Doppler frequency, τ : delay)

$$P_s(\nu, \tau) = \sum_{i,j} |S_{i,j}(\nu, \tau)|^2 \delta(\tau - \tau_i) \delta(\nu - \nu_j). \quad (1)$$

The average power delay profile (APDP), $P(\tau)$, also depends on the delayed and attenuated taps (τ_i, A_i):

$$P(\tau) = \sum_i \delta(\tau - \tau_i) \sum_j |S_{i,j}(\nu_j, \tau)|^2. \quad (2)$$

The excursion of the Doppler power spectrum $P_s(\nu, \tau_i)$ is identical for each tap and is given by the Clarke model [8]:

$$P_s(\nu, \tau_i) = \frac{A_i}{4\pi\nu_{max}} \frac{1}{\sqrt{1 - (\frac{\nu}{\nu_{max}})^2}}. \quad (3)$$

The ITU-R tapped delay line model [6] selection representative of an urban area (micro and small cells) is based on a comparison between urban measured propagation channels and filtered tapped delay line models (equivalent band for the comparison). A micro-cell (MC) environment is typical of a dense urban area with the base station (BS) height below the average rooftop-height of buildings while a small cell (SC) corresponds to BS height slightly higher than the rooftop-height of buildings [9]. We have evaluated the delay spread and the delay window set to 95% (W95%), after a pre-filtering processing (in a 25 MHz bandwidth and a roll-off equal to 0.61) applied on ITU-R models. The coherence bandwidth ($B_c - 0.5$) has been deduced from the OFDM dimensioning (section 2.2) used to sample the average frequency correlation function. Table 1 provides wideband selectivity parameters of outdoor ITU-R tapped delay line models and France Telecom R&D measurements carried out in MC and SC environments.

Table 1. wideband selectivity parameters in urban area

	Outdoor to Indoor and Pedestrians		Vehicular test Environment	
	A	B	A	B
1-ITU-channel				
delay spread (μs)	0.045	0.633	0.371	4.00
delay window 95% (μs)	0.20	2.35	1.16	12.94
$(B_c - 1/2)$ MHz	0.781	0.234	0.351	0.390
2-FT R&D channels	SC(1)	SC(2)	MC(1)	MC(2)
delay spread (μs)	0.44	0.673	0.186	0.271
delay window 95% (μs)	1.533	1.803	0.696	1.163

SC(1) and SC(2) scenarios are connected to SC cases with a distance range inferior to 500 m. while MC(1) and MC(2) describe MC cases covering up a 200-300 m distance range. Results show that the frequency selectivity significantly increases with the BS height. The delay spread for SC is twice as large as in MC. Table 1 and [7] show that the pedestrian A is related to large indoor areas and vehicular B to urban MC environments. Table 1 also confirms that the vehicular test environment A is rather attached to MC [7], while pedestrian B shall be related to either very selective macro-cell or SC environments. Hence, in the following, we select the vehicular test environment channel A to simulate a typical MC case and the pedestrian channel B environment to simulate a typical SC case. Relative delays and attenuations are reported in Table 2.

Table 2. Test Environments

Vehicular Test Environment (channel A)						Pedestrian Test Environment (channel B)					
Tap	Delay (μs)	Power (dB)	Tap	Delay (μs)	Power (dB)	Tap	Delay (μs)	Power (dB)	Tap	Delay (μs)	Power (dB)
1	0.0	0.0	4	1.09	-10.0	1	0.0	0.0	4	1.2	-8.0
2	0.31	-1.0	5	1.73	-15.0	2	0.20	-0.9	5	2.30	-7.8
3	0.71	-9.0	6	2.51	-20.0	3	0.80	-4.9	6	3.70	-23.9

2.2 OFDM system parameters

The conventional OFDM modulation set-up results in N_u overlapped sub-carriers with a transfer function of the k -th sub-carrier given by:

$$G_k(f) = T_u \delta(f - f_k) e^{j2\pi f T_u} \text{sinc}(\pi f T_u) \quad (4)$$

where T_u denotes the useful symbol duration. As shown in Fig. 1, transmitted QPSK data symbols are serial to parallel (S/P) mapped through N_u branches modulating N_u sub-carriers. The OFDM signal is obtained by an inverse fast Fourier transform (FFT) of length N_{fft} , with $N_{fft} > N_u$. A cyclic prefix (CP) of duration Δ is inserted at the beginning of each OFDM symbol to cancel intersymbol interference between successive OFDM symbols. The time-variant multipath propagation channel filters data. The received OFDM signal is the sum of a filtered version of the OFDM transmitted signal and of an additional Gaussian noise.

After removal of the CP, the OFDM demodulation, operated by an FFT, exploits the orthogonality between sub-carriers to estimate incoming data symbols. A perfect channel estimation is assumed. The OFDM parameter definition has then consisted in

adjusting Δ to the largest delay excursion trying also to minimize N_{fft} . Denoting by T_e the sampling period we, firstly, impose that: $T_u = p \cdot \Delta = N_{fft} T_e$.

Secondly, by refining the parameters p and N_u , we have adjusted the bandwidth B_w to the UMTS channelization in order to get a net bit rate (D_u) similar to the UMTS chip rate. At the end, in order to limit the spectrum efficiency loss (SEL), we have got $p = 8$. Denoting by R_c the code rate, corresponding to the channel code used for JSCD, and m the number of bits per subcarrier, we get

$$B_w = \frac{N_u}{T_u} = \frac{N_u}{p\Delta}, SEL = \frac{p}{p+1}, D_u = \frac{mR_c N_u}{(p+1)\Delta}. \quad (5)$$

Table 3 summarizes the OFDM parameter sets. They are slightly different for both environments along an accurate CP refinement intended to reduce the FFT size for each scenario. The parameter SEL is kept constant in order to allow a bit error rate (BER) comparison between MC and SC environments.

Table 3. System parameters

	Vehicular A	Pedestrian B
N_u : # of sub-carriers	112	145
ν_{max} : Doppler excursion (Hz)	89.6	89.6
$T_s = T_u + \Delta$: OFDM symb. duration (μs)	28.8	37.65
$\Delta = T_u/p$ (μs): Cyclic prefix duration	3.2	4.2
B_w : trans. bandwidth (MHz)	4.37	4.33
F_c : Sampling rate (MHz)/ N_{fft} : FFT size	5.62/144	5.71/191
T : Interleaver depth (ms)	14.45	14.45
D_u : Net bit rate (Mbps) ($R_c = 1/2, 1/3$)	(3.89, 2.59)	(3.85, 2.56)
$-SEL$ (dB)	0.51	0.51
Sub-carrier modulation	QPSK	QPSK

To test our JSCD technique, convolutional codes (CC) and turbo codes (TC) have been implemented. A pseudo-random binary interleaving (II) has been performed to cope with fast fading. The interleaving depth T , is much larger than the inverse positive Doppler excursion. An additional inner interleaving (frequency interleaving, not reported in Fig. 1) has also been applied within every OFDM symbol.

2.3 The JSCD technique

In [3], [10], [11], the authors propose a method to provide a low complexity JSCD of VLCs used in conjunction with convolutional or turbo codes. The key idea is to improve the channel decoding by using, at a bit level, an *a priori* source information. Assuming source symbols probabilities are known at the receiver, it is then possible to compute for each bit associated with a VLC tree branch, a source bit probability. By keeping a one-to-one correspondence between the VLC tree and the channel code trellis, these *a priori* bit probabilities can be inserted in the metrics of the channel decoding algorithm to improve the receiver performance. In the case where CC are used, the channel decoding is based on a sequence *maximum a posteriori* (MAP) algorithm. When TC are employed, it is a bit to bit MAP decoder that we are looking for. However, in this last case, in order to keep the complexity low when the *a priori* source information is taken into account, a

SUBMAP [12] is used instead of a BCJR [13]. As in most JSCD techniques applied on VLC, packetization is realized to limit the error propagation phenomena at some point. In [3], [10], [11], JSCD performances are given on the AWGN channel for different source statistics and different channel codes. Here, we also evaluate its performances over a time-variant multipath channel with an OFDM modulation.

3 Soft error pattern principle

The proposed JSCD method may only involve a slight modification in the computation of the channel code metrics at the decoder side. That means no additional delay and only a small extra computational cost. However its simulation over a multipath channel using OFDM modulation may be time consuming. Hence, it may be convenient to get the soft encoded metrics corresponding to long sequences of transmitted bits over the overall channel, including modulation. Then different configurations of source coding (with VLCs) and channel coding can be simply tested using the resulting soft error pattern file. Such procedures, leading to hard error patterns, are well known in the case of hard input-hard output channels. Here, we propose an extension leading to the concept of soft error pattern file, *i.e.* a file that contains real values representing all components between the channel coding output and the channel decoding input. Thus, for a given modulation scheme, a soft error pattern describes symbol decision errors on the encoded bits due to multipath degradations. In the following, the generation method, its use and validation, are illustrated in the case of two test environments, named vehicular A and pedestrian B (see Table 2).

3.1 Generation and use

Soft error pattern generation is deduced from the global transmission scheme depicted in Fig. 1. For each carrier-to-noise ratio (C/N), a soft error pattern file shall be generated and fed to various codec structures.

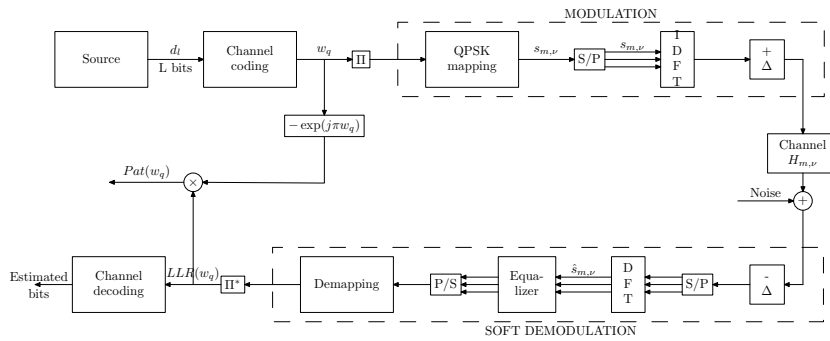


Fig. 1. OFDM transmission scheme through a time-variant multipath channel with soft error pattern generation.

The log likelihood ratios (LLRs) at the deinterleaver (II^*) output can be modelled by a sequence of real random variables (RVs). As a QPSK mapping is used, each coded bit after interleaving undergoes the same channel degradation. Then, the RVs can be viewed as identically distributed. We note LLR one RV of this sequence. For another mapping, one should consider as many RV as classes of LLRs with identical probability mass function (pmf). For example, for the 16 quadrature amplitude modulation (QAM) mapping, one should consider 2 RVs. We denote by w a uniformly distributed discrete RV with alphabet $\{0, 1\}$. It represents a bit at the channel coding output. As the QPSK mapping and the channel are symmetric, the pmf can be written as:

$$P(LLR|w = 0) = P(-LLR|w = 1), P(LLR|w = 1) = P(-LLR|w = 0). \quad (6)$$

Similarly to the LLRs, the soft error pattern can be modelled by a sequence of real and identically distributed RVs. We note Pat one of them, and we define it, as shown in Fig. 1, by: $Pat = -LLR \exp(j\pi w)$. Then, its pmf is such that: $P(Pat|w = 0) = P(-LLR|w = 0)$ and $P(Pat|w = 1) = P(LLR|w = 1)$. With equation (6), we get $P(Pat|w = 0) = P(Pat|w = 1) = P(Pat)$. Hence, the random variable Pat is independent of the transmitted bit. As illustrated in Fig. 2, to use the soft error pattern with a new source, we set: $LLR' = -Pat \exp(j\pi w')$. w' is a RV associated with a bit at the new channel code output and LLR' is the RV associated with the new LLR.

Then, the pmf of the RV LLR' is: $P(LLR'|w' = 0) = P(-Pat)$ and $P(LLR'|w' = 1) = P(Pat)$, since Pat is independent of w' .

Finally we get:

$$P(LLR'|w' = 0) = P(LLR|w = 0), P(LLR'|w' = 1) = P(LLR|w = 1). \quad (7)$$

These two last equations mean that for the two considered transmission schemes: the one in which all the components between channel coding and decoding are present and the one where they are replaced by the pattern, the LLRs have an identical pmf. Hence, this two schemes are equivalent. A soft error pattern is then a suitable way to represent the OFDM modulation and demodulation and the channel degradation. It is associated to a number of simulated bits, a C/N ratio, a given interleaver and a mapping. Its statistics do not depend on the channel and source codes used to generate it.

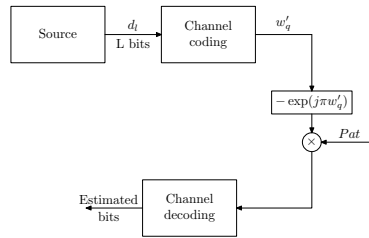


Fig. 2. Application of the soft error pattern.

3.2 Validation

To validate the soft error pattern process, we have compared the BER of the two systems: the overall transmission scheme presented in Fig. 1 and the simplified one proposed in Fig. 2, for several ratios of the useful bits energy over noise (E_b/N_0). The simulations have been run on the vehicular A channel using an *i.i.d* source and with CC of constraint length K equal to 9 for the UMTS channel codes of rate 1/2 and 1/3 [14], and to $K = 5$ for another CC. The octal representations of these CC are $(561, 753)_o$ and $(557, 663, 711)_o$ for the UMTS codes and $(31, 27)_o$ for the third CC. In Fig. 3 a) and b) the labels indicate, in first position, the channel code being used and in second position, when applicable, the CC used for generating the soft pattern files. This second indication also means that the results have been obtained running the simplified scheme with this CC. Otherwise the BER results from a simulation carried out using the overall OFDM transmission scheme.

In Fig. 3 a) it can be seen that we get similar results with the overall scheme and the simplified one, independently of the code rate used to generate patterns. Another validation is proposed in Fig. 3 b) with a pattern built using this time a UMTS CC ($K = 9, R_c = 1/2$) different from the CC ($K = 5, R_c = 1/2$) used for encoding the *i.i.d* source. Again the curves are superimposed showing that the pattern files accurately represent the vehicular A channel. A similar result, not reported here, also holds for the pedestrian B channel.

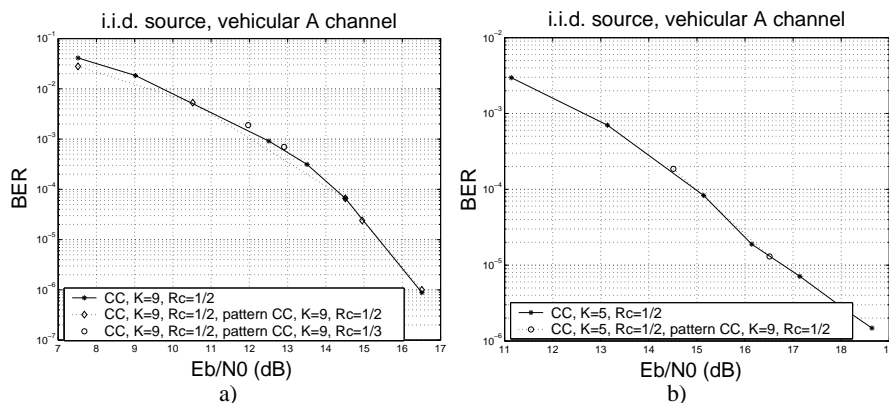


Fig. 3. “Soft error pattern” validation.

4 Results

4.1 JSCD performance with a convolutional code

In this section, the JSCD algorithm [3] recalled in section 2.3 is evaluated using the soft pattern files generated by the multipath OFDM radio transmission depicted in Fig. 1. We used the Huffman encoded first order Markov source proposed in [2]. The stationary and transition probabilities of this 3-symbol source are given in [11], its residual redundancy, defined by the difference between the VLC encoder’s code rate and the entropy

rate of the source, is 0.67. To limit the error propagation at a certain point, we have used resynchronization, packetizing data into blocks of 256 symbols. Our simulations correspond to the transmission of 5×10^7 coded bits, which is also the size of the soft error pattern file.

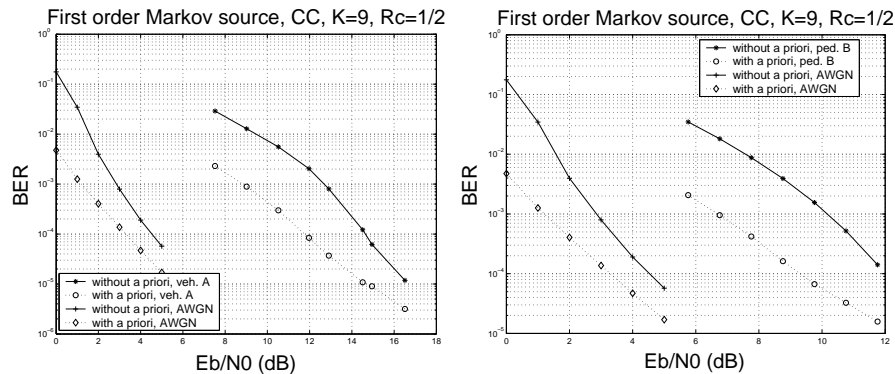


Fig. 4. BER with and without *a priori* source information for the first order Markov source of Murad and Fuja and a convolutional code $K = 9$, $R_c = 1/2$. Vehicular A channel on the left, pedestrian B channel on the right.

In a classical, or tandem, scheme the channel decoder does not use any *a priori* source information, while, as explained in subsection 2.3, for JSCD the *a priori* used are the VLC tree structure and the source statistics. In Fig. 4 these two approaches are compared, in terms of BER as a function of the E_b/N_0 , for the vehicular A and pedestrian B environments. These displays also include, as a matter of reference, our simulation results on the AWGN channel. The pedestrian B channel presents better performance than the vehicular A channel with a gain near 2 dB although the pedestrian B channel is the most frequency selective channel. This results shows that the OFDM dimensioning exploits in an efficient way the frequency selectivity of the propagation channel. For a BER of 10^{-4} , a gain of 3 dB, by using the JSCD technique, can be observed on both the vehicular A channel and the pedestrian B channel. Both displays also illustrate the fact that, compared to a tandem decoding, the impact of JSCD is still more important for mobile radio channels than for AWGN ones.

4.2 JSCD performance with turbo codes

In a second round of simulations we have used a UMTS turbo code [14]. This TC of rate 1/3 corresponds to a parallel concatenation of two systematic recursive coders, with generators $(13, 15)_o$. Contrary to the previous case, packets size is now given in bits and not in symbols. As we work with VLCs, it means that a packet does not obviously correspond to an integer number of symbols, so some extra bits are added to fill the packet. Here the packet size is chosen as 4096 bits, it is also the size of the internal line-column turbo code interleaver.

In Fig. 5 we show the results obtained at the third iteration of this turbo decoder for the vehicular A and pedestrian B channels. Results obtained with an AWGN transmis-

sion are also presented on the two corresponding displays. For a BER fixed to 10^{-4} , the improvement (in dB) obtained when using the *a priori* source information is around 2.4 dB on the pedestrian B channel and around 2.2 dB for the vehicular A channel.

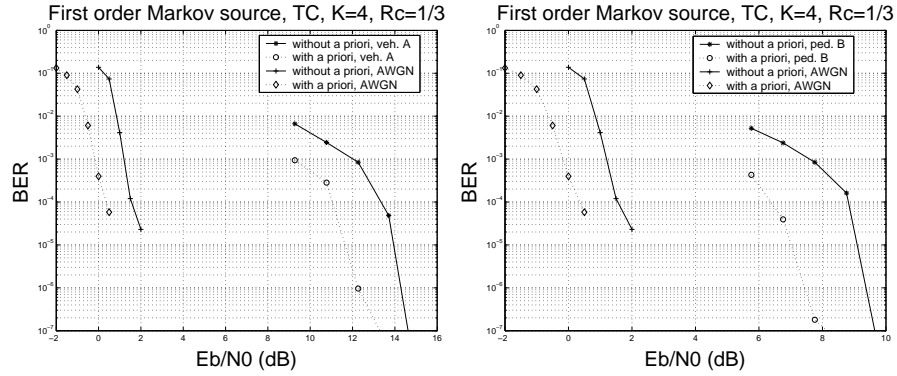


Fig. 5. BER with and without *a priori* source information for the first order Markov source of Murad and Fuja and a turbo code (3^{rd} iteration, $K = 4$, $R_c = 1/3$). Vehicular A channel on the left, pedestrian B channel on the right.

Another set of experiments has been carried out puncturing the TC output in order to get a code rate $R_c = \frac{1}{2}$. In Fig. 6 we can compare JSCD and tandem decoding for the two types of mobile environment and also in the case of the AWGN channel. For a BER fixed to 10^{-4} , the JSCD improvements in E_b/N_0 are 2.5 dB and 2.9 dB for the vehicular A channel and the pedestrian B channel, respectively. So, it can be

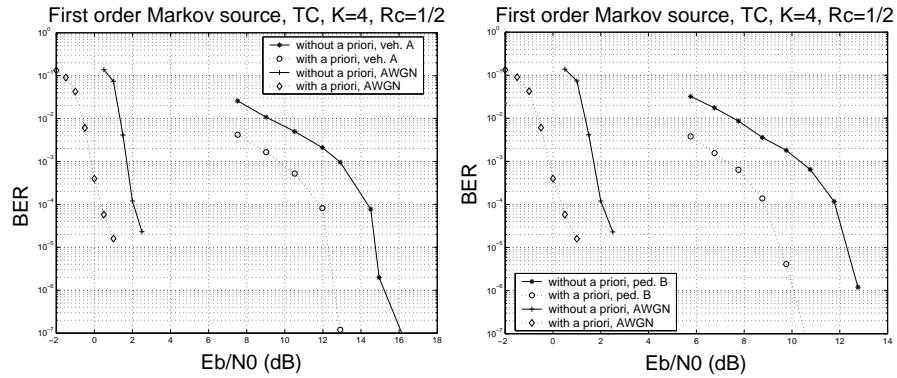


Fig. 6. BER with and without *a priori* source information for the first order Markov source of Murad and Fuja and a turbo code (3^{rd} iteration, $K = 4$, $R_c = 1/2$). Vehicular A channel on the left, pedestrian B channel on the right.

noted, at least in this case, that the positive impact of JSCD becomes stronger for lower channel code rates. Note also that, for both TC rates, the JSCD technique yields still more benefit in mobile environment than with the AWGN channel.

5 Conclusion

We have presented an application, in the context of FPLMTS, of a JSCD method for VLCs [3], [10], [11]. The channel modellization is based on ITU-R models [6] and France Telecom measurements [7], it also assumes an OFDM modulation which dimensioning has been carried out to fit to micro and small-cell areas. Results exhibit an efficient OFDM implementation in favour of a selective propagation channel attached to a small-cell area that should be translated into an extended radio coverage in the face of a micro-cell deployment. A soft error pattern generation is proposed that greatly simplifies the simulation of various JSCD techniques. When using convolutional codes or turbo codes borrowed from the UMTS standard [14], it is shown, with a Markov source [2], that thanks to our JSCD technique transmission gains between 2 and 3 dB are obtained.

References

1. Van Dyck, R.E., Miller, D.J.: Transport of wireless video using separate, concatenated, and joint source-channel coding. *Proceedings of the IEEE* **87** (1999) 1734–1749
2. Murad, A.H., Fuja, T.E.: Joint source-channel decoding of variable length encoded sources. In: *Proc. of ITW, Killarney, Ireland* (1998) 94–95
3. Guivarch, L., Carlach, J., Siohan, P.: Joint source-channel soft decoding of Huffman sources with Turbo-codes. In: *Proc. of DCC, Snowbird, Utah, USA* (2000) 83–92
4. Bauer, R., Hagenauer, J.: Iterative source/channel-decoding using reversible variable length codes. In: *Proc. of DCC, Snowbird, UT, USA* (2000) 93–102
5. Javaudin, J.P., Lacroix, D., Rouxel, A.: Pilot-aided channel estimation for OFDM/OQAM. In: *Proc. of VTC, Jeju, Korea* (2003) 1581–1585
6. International Telecommunication Union-Radio Study groups: Guidelines for evaluation of radio transmission technologies for imt-2000/fplmts. FPLMTS.REVAL, document 2/29-E (1996)
7. Yuan-Wu, Y., Siaud, I., Duponteil, D.: Radio performance evaluation of the DECT for WPCN based on ITU and recorded channel models. In: *Proc. of VTC, Ottawa, Canada* (1998)
8. Parsons, J.D.: *The mobile radio propagation channel*. Pentech-Press (1992)
9. Siaud, I.: A mobile propagation channel model with frequency hopping based on a digital signal processing and statistical analysis of wideband measurements applied in micro and small cells at 2.2 ghz. In: *Proc. of VTC, Phoenix, Arizona, USA* (1997)
10. Guivarch, L., Siohan, P., Carlach, J.: Low complexity soft decoding of Huffman encoded Markov sources using Turbo-codes. In: *Proc. of ICT, Acapulco, Mexico* (2000) 872–876
11. Jeanne, M., Carlach, J.C., Siohan, P., Guivarch, L.: Source and joint source-channel decoding of variable length codes. In: *Proc. of ICC. Volume 2., New York, USA* (2002)
12. Robertson, P., Villebrun, E., Hoeher, P.: A comparison of optimal and sub-optimal MAP decoding algorithms operating in the log-domain. In: *Proc. of ICC, Seattle, USA* (1995) 1009–1013
13. Bahl, L.R., Cocke, J., Jelinek, F., Raviv, J.: Optimal decoding of linear codes for minimizing symbol error rate. *IEEE Transactions on Information Theory* (1974) 284–287
14. 3rd Generation Partnership Project (3GPP): Technical Specification Group (TSG), Radio Access Network (RAN), Working Group 1 (WG1), Multiplexing and Channel Coding (FDD). TS 25 212 (1999)